

# Design and optimization of the magnetic circuit of a mobile nuclear magnetic resonance device for magnetic resonance imaging

**Abstract**—The resolution of magnetic resonance imaging, commonly known as MRI, depends on the homogeneity and field strength of the used primary magnetic field  $\vec{B}_0$  over the volume of interest. In clinical tomographs homogeneous fields are produced by solenoid coil windings or long round permanent magnets. These solutions are unsuitable for mobile usage because of weight and costs. This paper introduces an optimized magnetic circuit for a Mobile Universal Surface Explorer (MOUSE) which meets the requirements of sufficient homogeneity and low weight.

Keywords – Nuclear Magnetic Resonance, Magnetic Resonance Imaging, Mobile Universal Surface Explorer

## I. INTRODUCTION

The application of nuclear magnetic resonance (NMR) is based on the influence of an externally applied magnetic field  $\vec{B}_0$  on the nuclei' orientation. In the presence of an external field the magnetic moment  $\vec{\mu}$  will be aligned parallel or anti-parallel towards the  $\vec{B}_0$ -field and a resulting magnetization  $\vec{M}$  will occur. This magnetization precesses around the axis of the applied field with the Larmor frequency  $f_L = \frac{\gamma}{2\pi} B_0$  ( $\gamma$ : "gyromagnetic" ratio). The aligned magnetization vector can be excited by a high frequency pulse at the Larmor frequency. Only nuclei with  $f_L = \frac{\gamma}{2\pi} B_0$  will be affected.

Figure 1 shows the principle design of the MOUSE. The

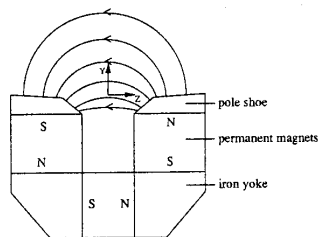


Fig. 1. Principle of the NMR-MOUSE

sample (e.g. human tissue, synthetic material) should be placed onto the measuring instrument. This design restriction causes an inhomogeneous field-strength distribution. The  $B_0$ -field decreases with increasing  $y$ -coordinate; the decrease of the field along the  $y$ -axis follows the equation  $B = B_0(y = 0) \cdot a^{-ky}$  with  $a > 1, k > 0$ . For magnetic resonance imaging a linear field gradient is required because only certain spins in selected slices  $\Delta y$  of the sample should be in resonance. In the case of the considered

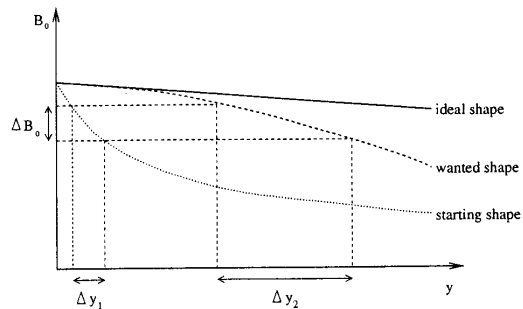


Fig. 2. Starting and wanted field-strength distribution in comparison to ideal homogeneity;  $\Delta B_0 = \frac{\Delta \omega}{\gamma} = \frac{\omega_1 - \omega_2}{\gamma}$

NMR-MOUSE the penetration depth is the  $y$ -axis. In the selected slice  $\Delta y$  only nuclei which meet the frequency requirement  $\Delta f = \frac{\gamma}{2\pi} \Delta B_0$  are excited by a high frequency pulse with the bandwidth  $\Delta f$ . Only these nuclei contribute to the test signal. Because of the wanted linear gradient there is a linear relationship between the bandwidth  $\Delta f$  and the slice thickness  $\Delta y$ .

A small linear gradient  $\frac{\Delta B_0}{\Delta y}$  of the main field  $B_0$  effects a small bandwidth  $\Delta f$  (corresponding to  $\Delta f \sim \Delta B_0$ ) field which is easier to produce. A high magnitude of  $B_0$  provides a better signal-to-noise-ratio because of the proportionality  $S \sim B_0^\lambda$  with  $1 < \lambda < 2$  [(K. H. Hausser, H. R. Kalbitzer, 1989)]. Besides a large gradient deteriorates depth of penetration. Figure 2 demonstrates the effect of non-linear  $B_0$ -field decrease on the depth of penetration. Either the required bandwidth  $\Delta f$  becomes larger for the same depth of penetration, or the selected slice-thickness becomes smaller for the same bandwidth ( $\Delta y_1 < \Delta y_2$ ). Therefore a linear field distribution with a small gradient is necessary at least over a short distance from the MOUSE surface. A small gradient, a high main field  $B_0$  and low weight of the magnetic circuit are the demands on the NMR-MOUSE.

For a detailed introduction to nuclear magnetic resonance (relaxation processes) and image reconstruction (two-dimensional Fourier imaging) it is referred to literature dealing with NMR and MRI [(J. Jin, 1999)], [(M. T. Vlaardingerbroeck, J. A. den Boer, 1996)], [(R. Kimmich, 1997)]. A description of hollow cylindrical tomographs for clinical applications can be found in [(H. Zijlstra, 1985)].

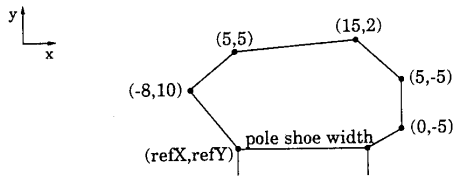


Fig. 3. Defining pole shoe shapes by using relative coordinates

## II. 2D CALCULATIONS

The following examinations are limited to 2D calculations and optimizations.

### A. Field calculations

The  $B_0$ -field is a pure static magnetic field and therefore the magnetic vector potential formulation  $\vec{B} = \nabla \times \vec{A}$  is used for solving the FEM-problem. This formulation is implemented in the solver of the commercial FEM-program ANSYS. ANSYS is used for the following presented results.

### B. $B_0$ -field influencing by pole shoe shapes

An empiric examination of different pole shoe shapes is hardly possible without a suitable aid because the pole shoe coordinates must be changed for each new pole shoe shape. A program automates this series (figure 3). The presented pole shoe shapes in figure 4 have a height of 10mm, the airgap is 45mm, the dimensions of the lower horizontal magnet are 45mm  $\times$  80mm, those of the vertical magnet are 80mm  $\times$  80mm. Figure 5 shows that the pole shoe shape does not affect the gradient of  $B_0$  in y-direction. The most suitable pole shoe geometries regarding a high flux density  $B_0$  are the models one and three (from the left side) in figure 4.



Fig. 4. A selection of different pole shoe shapes

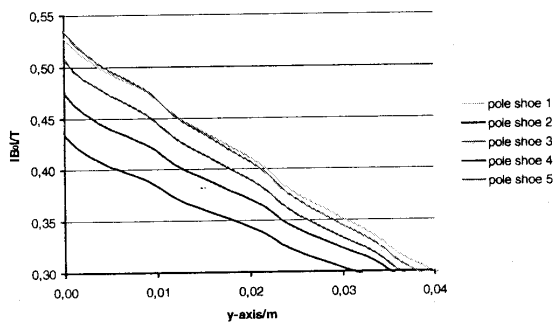


Fig. 5. Comparison of different pole shoe shapes

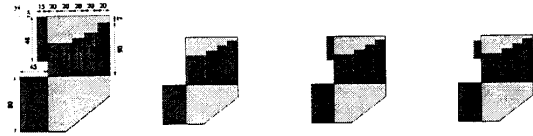


Fig. 6. Arrangements without and with (1,2) deflection magnets

## III. DEFLECTION MAGNETS

The results above demonstrate that a simple C-core with pole shoes upon the magnets does not affect the gradient. For this reason a deflection magnet (figure 6) which is magnetized in x-direction is attached in the airgap. By using deflection magnets it is possible to achieve an almost constant field distribution at least for the first 10mm in y-direction. The position of the deflection magnet in the airgap is important for the  $B_0$ -shape as it is shown in figure 7. This position has an effect on the gradient of  $B_0$  as well as on the induction value and can avoid a local maximum of  $B_0$ -field distribution which is in the way of image reconstruction. An optimization tool is used in order to find suitable dimensions of the used magnets.

## IV. DESIGN OPTIMIZATION

The optimal gradient shape combined with a high field strength is achieved by an optimization loop. The FEM-program ANSYS offers different optimization tools [(ans, )]. There are three types of optimization variables:

- The independent variables are called design variables.

$$\vec{x} = (x_1 \ x_2 \ \dots \ x_n) \quad (1)$$

They determine the geometry of the NMR-MOUSE such as magnets' height and width and position of the deflection magnet. Design variables can be changed by the optimization algorithm in order to fulfil certain requirements expressed by state variables. Design variables are restricted by lower and upper limits:

$$\underline{x}_i \leq x_i \leq \bar{x}_i \quad (i = 1, 2, \dots, n) \quad (2)$$

These limits depend on the allowed or wished dimensions of the NMR-MOUSE. For example: one aim of the optimized NMR-MOUSE is a certain weight that must be kept. For this reason there are certain design restrictions regarding the external dimensions of the MOUSE.

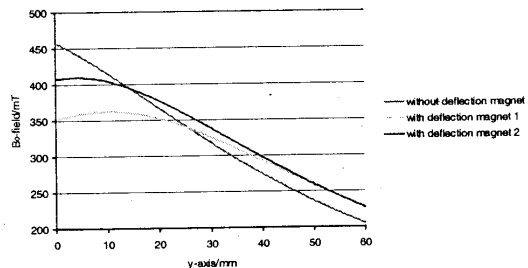


Fig. 7. Comparison of arrangements with deflection magnets

penetration depth/mm	infinite boundary elements	conventional boundary condition		
	$B_0/mT$	$B_0/mT$		
	30cm air	30cm	90cm	150cm
0	352,16	359,8	355,76	353,65
20	353,02	359,56	356	354,15
40	294,25	300,06	296,92	295,27

TABLE I

Comparison of 2D solutions with infinite boundary elements to 2D solutions with conventional boundary condition

penetration depth/mm	2D calculations	3D calculations		
	$B_0/mT$	$B_0/mT$		
		6cm	24cm	100cm
0	352,16	42,75	198,33	299,32
20	352,06	91,09	230,16	307,93
40	292,52	82,64	197,7	259,1

TABLE II

Comparison of different model depths for the NMR-MOUSE

- The optimization algorithm tries to minimize the objective function

$$f = f(\vec{x}) \quad (3)$$

so that state variables are kept. The objective function is a weighted function of the required gradients.

- The state variables are defined by the necessary field strength  $B_0(y_i)$  in a certain depth of penetration. The optimized magnetic circuit should supply required flux density within defined limits at  $y = 0mm$ ,  $y = 20mm$  and  $y = 40mm$ .

$$\underline{w}_i \leq w_i(\vec{x}) \leq \bar{w}_i \quad (4)$$

## V. VERIFICATION OF FEM CALCULATIONS' ACCURACY

A way of influencing the gradient of the NMR-MOUSE has been introduced for 2D calculations. In contrast to electrical machines there is a great airgap and no surrounding iron yoke. The accuracy of the FEM-calculations essentially depends on the amount of integrated air volume. An increasing number of air elements with  $\mu_R = 1$  decreases the induction value  $B_0$  along the y-axis. For this reason 2D and 3D infinite boundary elements are used. A verification of the FEM-calculated solution is the comparison of solutions with boundary elements to solutions with conventional triangular(2D)/tetrahedral(3D) elements and conventional boundary conditions ( $B_{normal} = 0$  on the boundary of the FEM domain). The solution with conventional boundary conditions should converge to that with infinite boundary elements if the integrated air volume expands. Table I verifies this assumption for penetration depths at  $y = 0mm$  (on the MOUSE surface),  $y = 20mm$  and  $y = 40mm$ .

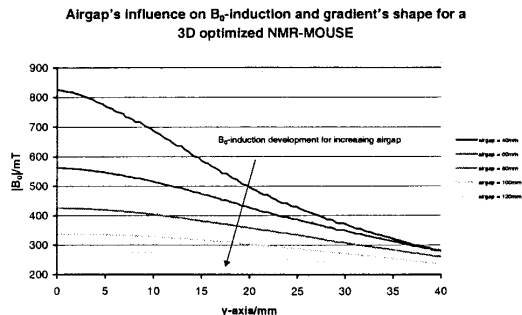


Fig. 8. Influence of the airgap of the NMR-MOUSE

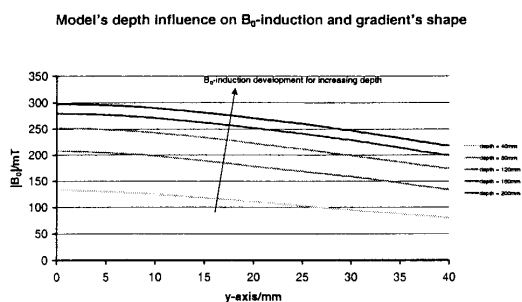


Fig. 9. Influence of the depth of the NMR-MOUSE

## VI. 3D CALCULATIONS

### A. Elimination of stray flux

A large problem of 3D calculations is the appearing stray flux in z-direction. Table II shows the influence of model's depth. For these calculations the introduced 2D arrangement with deflection magnets within the airgap was maintained and only extruded in z-direction. One can draw the conclusion that two dimensional optimizations are insufficient for the NMR-MOUSE because of the amount of surrounding air. There are two main parameters which influence the stray flux and the gradients' shape:

- The airgap influences the gradient's shape; a larger airgap provides a linear gradient shape (fig. 8).
- The depth of the NMR-MOUSE decreases the stray flux' effect on  $B_0$ -induction along the y-axis (fig. 9).

Therefore the two dimensionally found geometry with deflection magnets and the position of the deflection magnets within the airgap must be slightly modified. Figure 10 shows the principle design of the modified prototype.

The plain iron pole shoe is necessary in order to avoid a local maximum of  $B_0$ -induction shape which is a strictly monotonic function as figure 11 demonstrates.

### B. Reduction of weight

The weight of this arrangement can be reduced by using highly remanent NdFeB magnets. Besides the demand

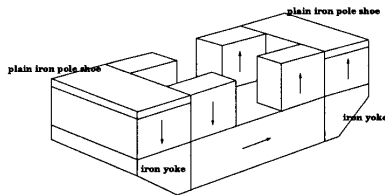


Fig. 10. Prototype of the NMR-MOUSE with modified deflection magnets

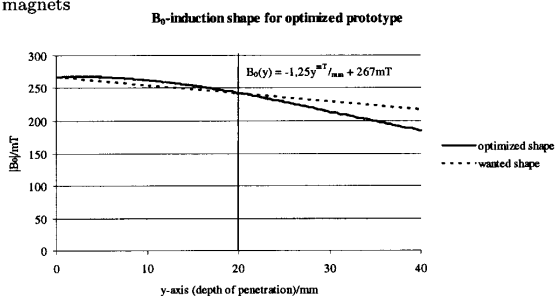


Fig. 11.  $B_0$ -induction shape for the optimized prototype

for low weight, a high magnitude of  $B_0$ -induction and a small gradient are contradictory. One can state that field strengths above  $B_0(y = 0) = 250\text{mT}$  and  $\frac{\Delta B_0}{\Delta y} = 1.25 \frac{T}{m}$  can only be realized with use of much magnetic material (>30kg). This weight and costs contradict the mobile application of the MOUSE. A possibility of reducing weight may be a cylindrical magnetic arrangement. The surrounding permanent magnets have a certain magnetization direction. On the one hand this arrangement reduces the total weight up to 50%, on the other hand it produces a tangential and not a normal field distribution concerning the y-axis.

## VII. CONCLUSION

In this paper a way of influencing the gradient and reducing stray flux and weight of the NMR-MOUSE has been introduced. 2D modelling and the use of pole shoes are unsuitable for this kind of application.

## REFERENCES

- ANSYS Advanced Analysis Techniques, Design Optimization.*
- H. Zijlstra (1985). Permanent magnet systems for NMR tomography. *Philips Journal of Research*, 40(5):259–288.
- J. Jin (1999). *Electromagnetic Analysis and Design in Magnetic Resonance Imaging*. CRC Press.
- K. H. Hausser, H. R. Kalbitzer (1989). *NMR für Mediziner und Biologen*. Springer-Verlag.

M. T. Vlaardingerbroeck, J. A. den Boer (1996). *Magnetic Resonance Imaging: Theory and Practice*. Springer-Verlag.

R. Kimmich (1997). *NMR, Tomography Diffusometry Relaxometry*. Springer-Verlag.